Quantum, many-body, finite-temperature perturbation theory for an electron-ion system

George A. Baker, Jr. and J. D. Johnson

Theoretical Division, Los Alamos National Laboratory

University of California, Los Alamos, N. M. 87544 USA

(845 July 1, 1999)

Abstract

The expansion in powers of the electron charge, e, for a neutral system of electrons (Fermions) and ions (Maxwell-Boltzmann particles) is extended to order e^4 for arbitrary values of temperature and density. The methods of calculation of the series terms will be illustrated, and some of the consequences of these results will be discussed. The ionization profile so derived, at least at high temperatures, will be contrasted with Saha theory. Some special features of hydrogen related to the possible plasma phase transition will be noted.

05.30.-d, 51.30.+i,05.70.-a,64.70.Fx

Typeset using REVTEX

I. INTRODUCTION

In this paper, we will first sketch the calculation of the pressure of a neutral, ion-electron gas as an expansion in powers of the electron charge e, by means of the Matsubara, finite-temperature, many-body, perturbation theory. For a full report on the expansion, see reference [1]. Much previous work has been done in this general area [2]. In this work we address the systematic expansion of the pressure of an electron-ion system [3], rather than a one-component plasma, in powers of the electron charge. This method of working is different in an important sense from much other work. It is based on the ideas of Taylor's theorem and of methods of analytic continuation. In the theory of critical phenomena, this method is a standard one [4], and has worked very well on a variety of lattice spin-models and other problems too. It has been used to determine the location and the nature of the critical point. We know from the theory of phase transitions that as the critical point is approached, the compressibility diverges, for example. We do not have enough terms actually to obtain good results very near the critical point, but as the divergence in the compressibility is normally manifest a considerable distance from the critical point, we will be able to see this early indicator of a possible phase transition. Often workers have looked for a low density expansion, or summed up what they deem to be the most important classes of diagrams that they were able to do. When used to study critical properties, this latter method has commonly been found to mischaracterize the nature of the critical point.

II. BACKGROUND

The starting Hamiltonian is

$$H = \sum_{i=1}^{ZN} \frac{p_i^2}{2m} + \sum_{j=1}^{N} \frac{P_j^2}{2M} + \sum_{i<j}^{ZN} \frac{e^2}{|\vec{r}_i - \vec{r}_j|} - \sum_{i}^{ZN} \sum_{j}^{N} \frac{Ze^2}{|\vec{r}_i - \vec{R}_j|} + \sum_{i<j}^{N} \frac{Z^2 e^2}{|\vec{R}_i - \vec{R}_j|}.$$

The key thermodynamic formulæ are [5]

$$p\Omega = kT \log \mathcal{Q}, \qquad \frac{\partial(-kT \log \mathcal{Q})}{\partial e^2} = e^{-2}\langle V \rangle,$$

where $\mathcal{Q}$ is the grand partition function.

Thus our basic formula is

$$p\Omega = \int_0^{e^2} e^{-2}\langle V \rangle \, de^2 + p_0\Omega.$$

For the Coulomb potential the wave number representation is $\tilde{v}(\vec{q}) = 4\pi e^2/q^2$.

In these diagrams the wavy lines represent the momentum transfer, the solid lines the fermions and the dashed lines the fermion holes. Each fermion line has a wave number $\vec{q}$, a frequency ω, and a factor of

$$\frac{e^{i\omega_n'\tau}}{i\omega_n' - \epsilon(\vec{p}\,') + \mu},$$

associated with it. Momentum and frequency are conserved at every vertex. The frequencies associated with the fermions are odd ($\omega_n = (2n+1)\pi$), and those with the momentum transfers are even.

In Fig. 1 we show the first order terms. The direct order e^2 term vanishes by electrical neutrality. In the exchange term, summing over the frequencies, we get

$$p_{E1} = -\frac{4\pi e^2}{(2\pi)^6} \int \frac{d\vec{k}_1 \, d\vec{k}_2}{(\vec{k}_1 - \vec{k}_2)^2} n(\vec{k}_1) n(\vec{k}_2).$$

In the second order in e^2 there are a number of cases to consider. The first is the direct term as shown in Fig. 2. It gives

$$-\frac{2(4\pi e^2)^2 (kT)^3}{(2\pi)^9} \sum_{\omega_1,\omega_2,\omega_3} \int \frac{d\vec{k}_1 \, d\vec{k}_2 \, d\vec{q}}{q^2 q^2} \Bigg[\frac{1}{i\omega_1 - \epsilon(\vec{k}_1) + \mu} \times \frac{1}{i\omega_2 - \epsilon(\vec{k}_2) + \mu} \frac{1}{i\omega_1 + i\omega_3 - \epsilon(\vec{k}_1 + \vec{q}) + \mu} \times \frac{1}{i\omega_2 - i\omega_3 - \epsilon(\vec{k}_2 - \vec{q}) + \mu} \Bigg].$$

Summing over ω_1, ω_2 we get

$$-\frac{kT}{2(2\pi)^3}\sum_{\omega_3}\int d\vec{q}\left[\frac{8\pi e^2}{q^2}\Xi(\vec{q},\omega_3)\right]^2,$$

where,

$$\Xi(\vec{q},\omega_3)=\frac{1}{(2\pi)^3}\int\frac{[n(\vec{k})-n(\vec{k}-\vec{q})]\,d\vec{k}}{-i\omega_3+\epsilon(\vec{k})-\epsilon(\vec{k}-\vec{q})}.$$

The Gell-Mann Brueckner trick [6] to handle this divergent term is to sum over the ring diagrams before doing the integral over $\vec{q}$. The third order ring diagram is shown in Fig. 3. It gives

$$-\frac{kT}{2(2\pi)^3}\sum_{\omega_3}\int d\vec{q}\left[\frac{8\pi e^2}{q^2}\Xi(\vec{q},\omega_3)\right]^3.$$

The series is just a geometric one, and so the contribution to $\langle V\rangle$ sums to

$$-\frac{kT}{2(2\pi)^3}\sum_{\omega_3}\int d\vec{q}\left\{\frac{[8\pi e^2\Xi(\vec{q},\omega_3)]^2}{q^2-8\pi e^2\Xi(\vec{q},\omega_3)}\right\}.$$

in which the integration over $d\vec{q}$ is no longer singular, however as we will see below, this term is now proportional to e^3 instead of e^4 its nominal order. When integrated with respect to de^2 this term for $p\Omega$ becomes

$$-\frac{kT}{2(2\pi)^3}\sum_{\omega_3}\int d\vec{q}\left\{\ln\left[1-\frac{8\pi e^2}{q^2}\Xi(\vec{q},\omega_3)\right]\right.$$
$$\left.+\frac{8\pi e^2}{q^2}\Xi(\vec{q},\omega_3)\right\}.$$

This is the famous Debye-Hückel term. The sum of the ring diagrams in leading order in e and including the ion-ion, electron-electron, and ion-electron effects is

$$p_{DH}=-\frac{kT}{(2\pi)^2}\left(\frac{\pi}{3}\right)\left[\frac{4\pi Z^2Ne^2}{kT\Omega}\right.$$
$$\left.+\frac{e^2}{(2\pi)^2kT}\int d\vec{k}\,\mathrm{sech}^2\left(\frac{\epsilon(\vec{\mathrm{k}})-\mu}{2\mathrm{kT}}\right)\right]^{3/2}.$$

The next order corrections are e^4 and not just e^5.

The remaining, necessary second order diagrams in e^2 are shown in Figs. 4 and 5. Of these only E_{2a} and E_{2b} contribute as the rest vanish by electrical neutrality. The work in producing formulæ for these terms is similar to that given above, but more lengthy and a great deal more tedious.

The next step is to expand everything in sight in terms of the electron and ion fugacities, $z = \exp(\mu/kT)$, $z_{\rm ion} = \exp(\mu_{\rm ion}/kT)$. We use E_{2b} as an illustration. The integral formula here is,

$$p_{E2b} = -\frac{(4\pi e^2)^2}{2^3 kT(2\pi)^9}\left(\frac{2mkT}{\hbar^2}\right)^{5/2}\int \frac{d\vec{k}_1\, d\vec{k}_2\, d\vec{k}_3}{(\vec{k}_2-\vec{k}_1)^2(\vec{k}_1-\vec{k}_3)^2}$$
$$\times \frac{\mathrm{sech}^2\left(\frac{1}{2}\mathrm{k}_1^2 - \frac{\mu}{2\mathrm{kT}}\right)}{\left[1+\exp\left(k_2^2-\frac{\mu}{kT}\right)\right]\left[1+\exp\left(k_3^2-\frac{\mu}{kT}\right)\right]}.$$

We ignore the ion-ion term as relatively small. Let us make the change of variables $\vec{p}_1 = \vec{k}_2 - \vec{k}_1$ and $\vec{p}_2 = \vec{k}_3 - \vec{k}_1$. If we now expand this equation in powers of z we obtain,

$$4\sum_{j_1,j_2,j_3=1}^{\infty} j_3(-1)^{j_1+j_2+j_3-3} z^{(j_1+j_2+j_3)}$$
$$\times \int \frac{d\vec{p}_1\, d\vec{p}_2}{p_1^2 p_2^2} d\vec{k}_1\, \exp(-j_1 p_1^2 - j_2 p_2^2$$
$$-(j_1+j_2+j_3)k_1^2 - 2j_1\vec{p}_1\cdot\vec{k}_1 - 2j_2\vec{p}_2\cdot\vec{k}_1).$$

If we integrate over $\vec{k}_1$ by completing the square in Cartesian coordinates, then this equation becomes,

$$4\pi^{\frac{3}{2}}\sum_{j_1,j_2,j_3=1}^{\infty}\frac{j_3(-1)^{j_1+j_2+j_3-3}z^{(j_1+j_2+j_3)}}{(j_1+j_2+j_3)^{\frac{3}{2}}}\int\frac{d\vec{p}_1\, d\vec{p}_2}{p_1^2p_2^2}$$
$$\times\exp\left(\frac{-j_1(j_2+j_3)p_1^2 - j_2(j_1+j_3)p_2^2 + 2j_1j_2\vec{p}_1\cdot\vec{p}_2}{j_1+j_2+j_3}\right).$$

If we integrate over all the angles except that between $\vec{p}_1$ and $\vec{p}_2$ and denote the cosine of that angle by τ, then if we integrate over the magnitudes in the standard way for a quadratic form in the exponent, we get

$$8\pi^3\pi^{\frac{3}{2}}\sum_{j_1,j_2,j_3=1}^{\infty}\frac{j_3(-1)^{j_1+j_2+j_3-3}z^{(j_1+j_2+j_3)}}{j_1j_2(j_1+j_2+j_3)^{\frac{1}{2}}}$$
$$\times\int_{-1}^{1}\frac{\sqrt{j_1j_2}d\tau}{(j_3(j_2+j_1)+j_3^2+j_1j_2(1-\tau^2))^{\frac{1}{2}}}.$$

The final integral can now be evaluated to yield,

$$16\pi^{\frac{9}{2}}\sum_{j_1,j_2,j_3=1}^{\infty}\frac{j_3(-1)^{j_1+j_2+j_3-3}z^{(j_1+j_2+j_3)}}{j_1j_2(j_1+j_2+j_3)^{\frac{1}{2}}}$$
$$\times\sin^{-1}\left(\sqrt{\frac{j_1j_2}{(j_1+j_3)(j_2+j_3)}}\right),$$

Then we solve the thermodynamic equations,

$$\begin{aligned}
\frac{p\Omega}{kT} &= \log \mathcal{Q}(\Omega, T, z, z_{\rm ion}), \\
ZN &= z\frac{\partial}{\partial z} \log \mathcal{Q}(\Omega, T, z, z_{\rm ion})\Big|_{\Omega, T, z_{\rm ion}}, \\
N_{\rm ion} &= z_{\rm ion}\frac{\partial}{\partial z_{\rm ion}} \log \mathcal{Q}(\Omega, T, z, z_{\rm ion})\Big|_{\Omega, T, z},
\end{aligned}$$

and re-express the coefficients in terms of the dimensionless de Broglie density ζ, which is independent of the electron charge. The expansion is in terms of the dimensionless electron charge y.

$$\zeta = \frac{ZN}{2\Omega}\left(\frac{h^2}{2\pi mkT}\right)^{\frac{3}{2}}, \quad y^2 = \frac{e^2}{r_b kT}, \quad r_b = \left[\frac{3\Omega}{4\pi N}\right]^{\frac{1}{3}}.$$

This work is straightforward, but again lengthy and tedious. Finally it remains to provide convenient computational expressions for the various infinite series we have obtained in ζ. To do this we first revert the series expansion,

$$\zeta = \sum_{l=1}^{\infty} \frac{(-1)^{l+1} z^l}{l^{\frac{3}{2}}},$$

to give $z(\zeta)$, and then back substitute to give series expansions in powers of ζ. In our sample case, we form Padé approximants [7] to the series and get,

$$\begin{aligned}
&\int \frac{d\vec{k}_1\, d\vec{k}_2\, d\vec{k}_3}{(\vec{k}_2 - \vec{k}_1)^2(\vec{k}_1 - \vec{k}_3)^2} \\
&\times \frac{\operatorname{sech}^2\left(\frac{1}{2}\mathrm{k}_1^2 - \frac{\mu}{2\mathrm{kT}}\right)}{\left[1 + \exp\left(k_2^2 - \frac{\mu}{kT}\right)\right]\left[1 + \exp\left(k_3^2 - \frac{\mu}{kT}\right)\right]} \\
&\approx 16\pi^{\frac{9}{2}} \frac{\mu_6(\zeta)}{\theta_5(\zeta)}
\end{aligned}$$

to an accuracy of 0.1% for the integral, where,

$$\mu_6(\zeta) = 0.30229989\zeta^3 + 5.0287616 \times 10^{-2}\zeta^4$$

$$+3.6103004 \times 10^{-3}\zeta^5 + 1.0210313 \times 10^{-4}\zeta^6,$$

$$\theta_5(\zeta) = 1 + 1.2478566\zeta + 0.55778521\zeta^2 + 0.10432105\zeta^3$$

$$+7.2823921 \times 10^{-3}\zeta^4 + 2.1384429 \times 10^{-4}\zeta^5,$$

where use has been made of the result that this quantity is asymptotic to $24\pi^{\frac{7}{2}}\zeta$ as $\zeta \to \infty$. The other quantities can be represented in the same way, with more or less the same degree of difficulty.

III. HYDROGEN AND A POSSIBLE PLASMA PHASE TRANSITION

If we put all our results together, then we have the series expansion

$$\frac{P\Omega}{NkT} = G_0(\zeta) + G_2(\zeta)y^2 + G_3(\zeta)y^3 + G_4(\zeta)y^4 + o(e^4),$$

where the series coefficients are give explicitly by relatively messy expressions in terms of ζ. Graphically, we have G_0, the ideal Fermi gas curve, in Fig. 6.

In Fig. 7 we have the ratio G_2/G_0. In Fig. 8 we have G_3/G_0, and in Fig. 9 we plot G_4/G_0.

The results plotted in Fig. 10 show that the wrinkles in the curves interpolated from the series line up nicely with the critical point estimates given in references [8] and [9]. It supports, but of course does not prove, the existence of such a phase transition.

The misalignment (seen before) of the value of ζ for which the ideal Fermi gas function, (Pauli principle) and the Debye-Hückel function make their big changes in behavior is what causes the wrinkle in the contours previous shown, and presumably is what drives the phase transition (if it exists). This effect is too small to cause a similar effect in Lithium or any $Z \geq 3$, and is dubious for Helium.

IV. COMPARISON WITH SAHA THEORY

From the series expansion in e^2 we can compute the early terms of the low-density expansion:

$$\frac{p\Omega}{NkT} = 1 + Z\Bigg\{1 - \zeta^{\frac{1}{2}}\left[\frac{\sqrt{2\pi}}{3}(Z+1)^{\frac{3}{2}}\epsilon^3 + \ldots\right]$$
$$+ \zeta\left[\frac{1}{2^{\frac{5}{2}}} - \frac{1}{2}\epsilon^2 + \right.$$
$$\left.\left(\frac{\pi \ln 2}{2\sqrt{2}} + \frac{\pi\sqrt{2}}{4} - \frac{\pi}{2}Z - \frac{\pi\sqrt{2}}{4}Z^2\left(\frac{m}{M}\right)^{\frac{1}{2}}\right)\epsilon^4 + \ldots\right]$$
$$+ \zeta^{\frac{3}{2}}\left[\frac{3\sqrt{\pi}}{2}(Z+1)^{\frac{1}{2}}\epsilon^3 + \ldots\right] + o\left(\zeta^{\frac{3}{2}}\right)\Bigg\},$$

where $\epsilon \propto T^{-\frac{1}{4}}$, independent of density. This equation is the low-density limit of the ionization profile, at least for high temperatures.

In Saha theory [10] it is usual to take the degree of ionization to be proportional to the electron pressure; dividing the electron pressure by the ideal electron gas pressure, we deduce,

$$\lim_{r_b \to \infty} \frac{1 - \frac{Z_i}{Z}}{\left[(Z+1)\frac{a_0}{r_b}\right]^{\frac{3}{2}}} = \sqrt{\frac{2}{3}Z}\left(\frac{13.6052}{T_{\mathrm{ev}}}\right)^{\frac{3}{2}},$$

where a_0 is the Bohr radius. By contrast, the Saha formula

$$\frac{Z_i}{Z} = \frac{1}{1 + A\zeta\exp(\chi/T)}$$

gives

$$1 - \frac{Z_i}{Z} \propto \frac{\rho}{T^{\frac{3}{2}}}, \quad \text{instead of} \quad \propto \frac{\rho^{\frac{1}{2}}}{T^{\frac{3}{2}}},$$

given by the exact expansion. Here ρ is the electron density. The difference is a significant effect of quantum long range forces.

REFERENCES

[1] G. A. Baker, Jr., J. D. Johnson, J. D., Physica A **265**, 129 (1999).

[2] See for example, E. M. Montroll, J. C. Ward, Phys. Fluids **1**, 55 (1958); W. D. Kraeft, W. Stolzmann, Physica A **97**, 306 (1979); A. Alastuey and A. Perez, Europhys. Lett. **20**, 19 (1992); J. Riemann, M. Schlanges, H. E. DeWitt, W. D. Kraeft, Physica A **219**, 423 (1995).

[3] A. A. Bedenov, Soviet Physics, JEPT **9**, 446 (1959).

[4] C. Domb and M. S. Green, eds., *Phase Transitions and Critical Phenomena, Vol. 3*, (Academic Press, London, 1974).

[5] L. D. Landau and E. M. Lifshitz, *Course of Theoretical Physics, Vol. 5, Statistical Physics* as transl. E. Peierls and R. F. Peierls (Addison-Wesley, Reading, MA, 1958).

[6] M. Gell-Mann and K. Brueckner, Phys. Rev. **106**, 369 (1957).

[7] G. A. Baker, Jr. and P. R. Graves-Morris *Encyclopedia of Mathematics and its Applications, Vol. 59, Padé Approximants, second edition*, G.-C. Rota, ed. (Cambridge Univ. Press, New York, 1996).

[8] G. A. Baker, Jr., Phys. Rev. E **56**, 5216 (1997).

[9] R. Redmer, Zeit. für Phys. Chem. **204**, 135 (1998).

[10] N. H. Saha, Phil. Mag. **40**, 472 (1920); D. Mihalas, *Stellar Atmospheres* (W. H. Freeman, San Francisco, 1970).

FIGURES

FIG. 1. The diagrams for the first-order interaction in e^2.

FIG. 2. The second-order, direct-interaction diagram.

FIG. 3. The third-order ring diagram.

FIG. 4. The second-order, exchange-interaction diagram.

FIG. 5. The second-order, "forbidden diagram" and its exchange variants.

FIG. 6. The ideal, Fermi-gas curve versus the de Broglie density.

FIG. 7. The ratio of G_2/G_0. The large dot marks the projected critical value of ζ.

FIG. 8. The ratio of the Debye-Hückel term to the ideal Fermi gas term, G_3/G_0.

FIG. 9. The ratio of G_4/G_0. The large dot marks the projected critical value of ζ.

FIG. 10. Contours of $G_3 y^3/G_0$. The dashed line is is the 0.1% contour, the short-dashed line is for 1% and the dotted line is for 10%. The large dots are estimates of the critical point. The series projection of the critical point lies outside the range of validity of the series.

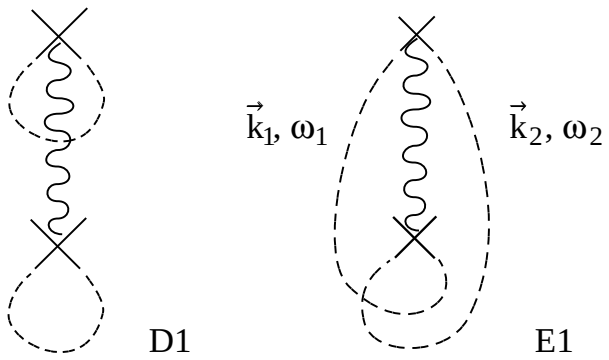

Figure 1

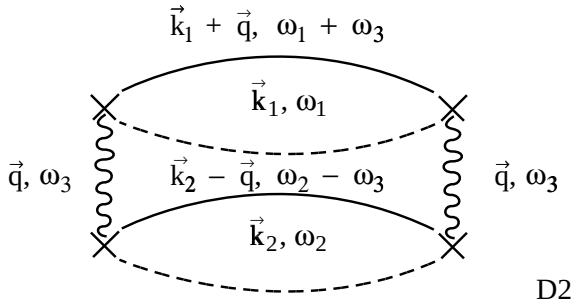
$\vec{k}_1 + \vec{q},\ \omega_1 + \omega_3$
$\vec{k}_1, \omega_1$
$\vec{q}, \omega_3$
$\vec{k}_2 - \vec{q},\ \omega_2 - \omega_3$
$\vec{q}, \omega_3$
$\vec{k}_2, \omega_2$
D2

Figure 2

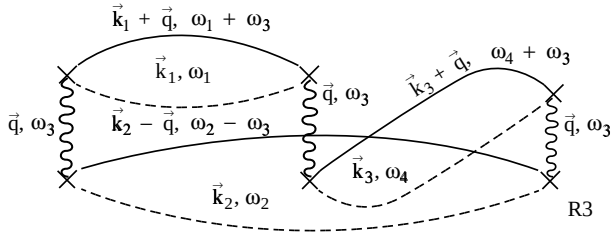
$\vec{k}_1 + \vec{q},\ \omega_1 + \omega_3$
$\vec{k}_1, \omega_1$
$\vec{q}, \omega_3$
$\vec{k}_2 - \vec{q},\ \omega_2 - \omega_3$
$\vec{q}, \omega_3$
$\vec{k}_2, \omega_2$
$\vec{k}_3 + \vec{q},\ \omega_4 + \omega_3$
$\vec{k}_3, \omega_4$
$\vec{q}, \omega_3$
R3

Figure 3

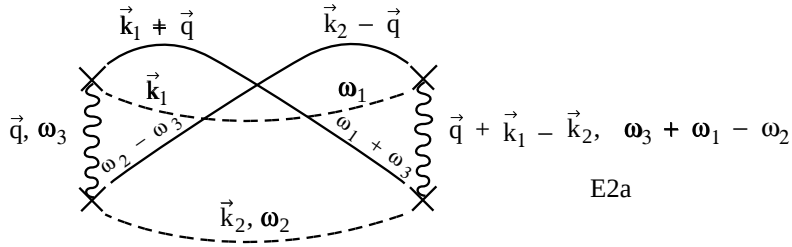
$\vec{k}_1 + \vec{q}$
$\vec{k}_2 - \vec{q}$
$\vec{k}_1$
ω_1
$\vec{q}, \omega_3$
$\omega_2 - \omega_3$
$\omega_1 + \omega_3$
$\vec{q} + \vec{k}_1 - \vec{k}_2, \quad \omega_3 + \omega_1 - \omega_2$
E2a
$\vec{k}_2, \omega_2$

Figure 4

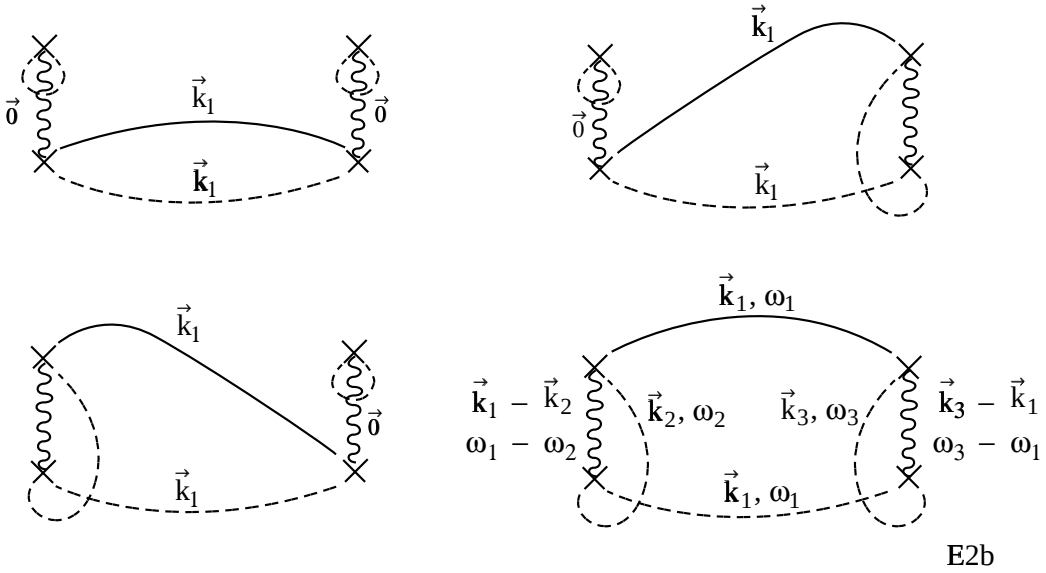
$\vec{0}$
$\vec{k}_1$
$\vec{0}$
$\vec{k}_1$
$\vec{k}_1$
$\vec{0}$
$\vec{k}_1$
$\vec{k}_1$
$\vec{0}$
$\vec{k}_1$
$\vec{k}_1, \omega_1$
$\vec{k}_1 - \vec{k}_2$
$\omega_1 - \omega_2$
$\vec{k}_2, \omega_2$
$\vec{k}_3, \omega_3$
$\vec{k}_3 - \vec{k}_1$
$\omega_3 - \omega_1$
$\vec{k}_1, \omega_1$
E2b

Figure 5

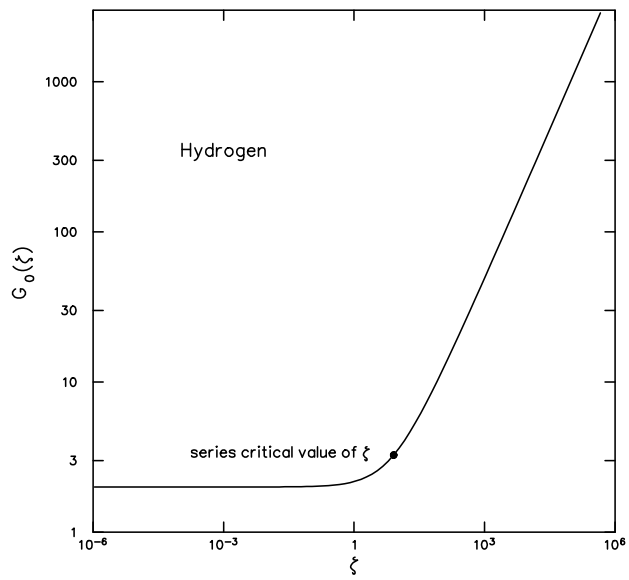
Hydrogen
series critical value of ζ
G0(ζ)
ζ
1000
300
100
30
10
3
1
10−6
10−3
1
103
106

Figure 6

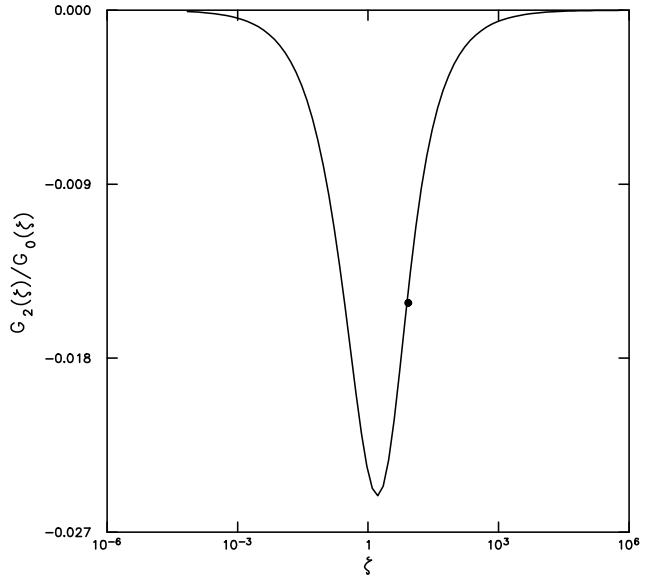

Figure 7

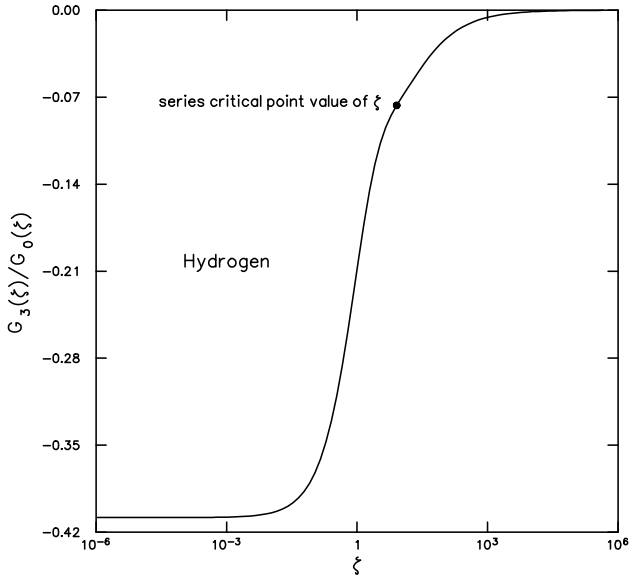
0.00
−0.07
−0.14
−0.21
−0.28
−0.35
−0.42
series critical point value of ζ
Hydrogen
G3(ζ)/G0(ζ)
10−6
10−3
1
103
106
ζ

Figure 8

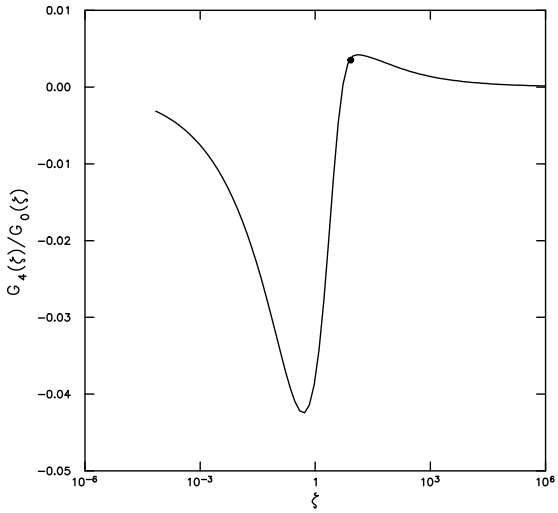
0.01
0.00
−0.01
−0.02
−0.03
−0.04
−0.05
$G_4(\zeta)/G_0(\zeta)$
10^{-6}
10^{-3}
1
10^{3}
10^{6}
ζ

Figure 9

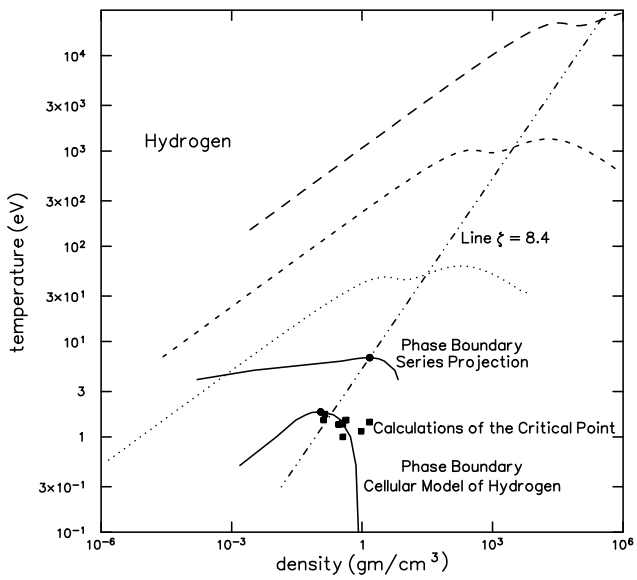
Hydrogen
Line ζ = 8.4
Phase Boundary
Series Projection
Calculations of the Critical Point
Phase Boundary
Cellular Model of Hydrogen
temperature (eV)
density (gm/cm 3)
10⁴
3×10³
10³
3×10²
10²
3×10¹
10¹
3
1
3×10⁻¹
10⁻¹
10⁻⁶
10⁻³
1
10³
10⁶

Figure 10